

Chapter 2

Pairing with transfer

2.1 Nuclear Structure in a nutshell

The low-energy properties of the finite, quantal, many-body nuclear system, in which nucleons interact through the strong force of strength $v_0 (\approx -100 \text{ MeV})$ and range $a (\approx 0.9 \text{ fm})$ are controlled, in first approximation, by independent particle motion. This is a consequence of the fact that nucleons display a sizable value of the quantal zero point (kinetic) energy of localization ($\hbar^2/Ma \approx 50 \text{ MeV}$) as compared to the absolute value of the strength of the NN -potential¹ $|v_0| = 100 \text{ MeV}$

The corresponding ground state $|HF\rangle = \prod_i a_i^\dagger |0\rangle$ describes a step function in the probability of the occupied ($\epsilon_i \leq \epsilon_F$) and empty ($\epsilon_k > \epsilon_F$) states, displaying a sharp discontinuity at the Fermi energy and thus $Z_\omega = 1$. Pushing the system it reacts with an inertia AM , sum of the nucleon masses (App. 1.D). Setting it into rotation, assuming the density $\rho(r) = \sum_i |\langle \mathbf{r}|i\rangle|^2$ ($|i\rangle = a_i^\dagger |0\rangle$) to be spatially deformed, it responds with the rigid moment of inertia. This is because the single-particle orbitals are solidly anchored to the mean field (Fig. 2.3.3).

Pairing acting on nucleons moving in time reversal states $\nu, \bar{\nu}$ ($\nu \equiv (nlj)$), in configurations of the type $((l)_{L=0}^2, (s)_{S=0}^2)$, and lying close to the Fermi energy $\epsilon_F (\approx 36 \text{ MeV})$, alter this picture in a conspicuous way². Within an energy range of the order of the absolute value of the pair correlation energy³ $|E_{corr}| (\approx 3 \text{ MeV})$

¹The corresponding ratio $q = \left(\frac{\hbar^2}{Ma^3}\right) \frac{1}{|v_0|}$ is known as the quantity parameter and was first used in connection with the study of condensed matter (de Boer (1948, 1957); de Boer and Lundbeck (1948); Nosanow (1976)). It was introduced in nuclear physics in Mottelson (1998) where its value $q = 0.5$ testifies to the validity of independent particle motion. It is of notice that questions like the one posed in connection with localization and long mean free path were already discussed by Lindemann (1910) in connection with the study of the stability or less of crystals. The generalization to aperiodic crystals, like e.g. proteins (Schrödinger, E. (1944)) was carried out in Stillinger and Stillinger (1990). Its possible application to the atomic nucleus is discussed in App. 2.C

²Bohr et al. (1958); for a recent compilation of ongoing research in the field see Broglia, R. A. and Zelevinsky, V. (2013).

³In BCS, $E_{corr} \approx -\frac{N(0)}{2} \Delta^2$, where $N(0) = \frac{g}{2}$ is the density of states at the Fermi energy and for one spin orientation, $g_i = i/16 \text{ MeV}^{-1}$ ($i = N, Z$) being the result of an empirical estimate which takes

$T \approx T_c$, (critical normal-superconducting temperature) they play an important role in normal (non-superfluid) nuclei. In particular in nuclei around closed shells (Fig. 2.1.1), and specially in the case of light, highly polarizable, exotic halo nuclei¹¹. From this vantage point one can posit that it is not so much, or, at least not only, the superfluid phase which is abnormal in the nuclear case, but the normal state around closed shell systems¹². In particular in connection with the self-energy of nucleons moving around closed shells¹³. It is of notice nonetheless, the role pairing vibrations play in the transition between superfluid and normal nuclear phases (cf. Fig. 2.1.2) as a function of the rotational frequency (angular momentum) as emerged from the experimental studies of high spin states carried out by, among others, Garrett and collaborators¹⁴.

From Fig. 2.1.2 it is seen that while the (dynamic) pairing gap associated with pairing vibrations leads to a $\approx 20\%$ increase of the static pairing gap for low rotational frequencies, it becomes the overwhelming contribution above the critical frequency¹⁵. In any case, the central role played by pairing vibrations within the present circumstances is that to restore particle-number conservation, another example after that provided by the quantity parameter and by its generalization to pair motion, of the fact that potential functionals are, as a rule, best profited by special arrangements of fermions (spontaneous symmetry breaking), while fluctuations favour symmetry¹⁶.

Within this context, there are a number of methods which allows one to go beyond BCS mean-field approximation, or of its generalization known as the Hartree-Fock-Bogolyubov approximation (HFB). Generally referred to as number projection methods¹⁷(NP), they make use of a variety of techniques (Generator Coordinate Method, Pfaffians, etc.) as well as protocols (variation after projection, gradient method, etc.). The advantages of NP methods over the RPA is to lead to smooth functions for both the correlation energy and the pairing gap at the pairing phase transition between normal and superfluid phases. That is, between the pairing vibrational and pairing rotational schemes¹⁸.

In Fig. 2.1.3 we display the excitation function associated with the reaction

fluid ^3He see Wölfe, P. (1978).

¹¹ See Sects. 2.5 and 2.6; Bohr, A. and Mottelson (1975). Bès, D. R. and Broglia (1966). Högaasen-Feldman (1961), Schmidt, H. (1972), Schmidt, H. (1968), Barranco, F. et al. (2001), Potel, G. et al. (2013a), Potel et al. (2014).

¹² See Potel, G. et al. (2013a) and refs. therein. Also Potel, G. et al. (2013b) in connection with the closed shell system ^{132}Sn .

¹³ See e.g. Bès and Broglia (1971a,b,c).

¹⁴ Garrett (1985). See also Shimizu, Y. R. et al. (1989), Barranco et al. (1987) and Ch. 6 of Brink, D. and Broglia (2005).

¹⁵ Shimizu, Y. R. et al. (1989), Shimizu, Y. R. and Broglia (1990), Shimizu, Y. R. (2013). Dönau, F. et al. (1999) Shimizu, Y. R. et al. (2000).

¹⁶ Anderson and Stein (1984); Aderson (1976).

¹⁷ cf. Ring, P. and Schuck (1980), Egido, J. L. (2013), Robledo, R. M. and Bertsch (2013); cf. also Frauendorf, S. (2013), Ring, P. (2013), Heenen, P. H. et al. (2013), and references therein.

¹⁸ Figs. 2.1.1, 2.1.3, 2.1.4, see also Fig. 2.4.1 and Sects. 2.4.2 and 2.5. cf. Bès, D. R. and Broglia (1966), Bohr, A. and Mottelson (1975) and references therein.

J.D. Garrett, G.B. Hagemann and B. Herskind,
Recent Nuclear Structure Studies of Rapidly Rotating
Nuclei, Ann. Rev. Nucl. Part. Sci., 36, 419 (1986)

$^{122}\text{Sn}(p, \tau)^{120}\text{Sn}(J^\pi)$, populating the low-energy states of the single open shell neutron superfluid nucleus ^{120}Sn . The angle selected to report the value of the absolute differential cross sections, that is 5° , corresponds to the first, and largest, peak of the absolute $L = 0$ differential two-nucleon transfer cross section. Essentially all the strength is concentrated in the ground state, the strongest 0^+ -excited state carrying a cross section of the order of 3% of that of the ground state. Within this context, the difference with the results displayed in Fig. 2.1.1 is apparent.

In the inset to Fig. 2.1.3 a quantity closely related to the Sn-isotopes binding energy is displayed (bold face levels). Namely $B(^{50+N}\text{Sn}_N) - 8.124N$ MeV + 46.33 MeV, obtained by subtracting the contribution of the single nucleon addition to the nuclear binding energy. The linear function in N was obtained by a linear fitting of the binding energies of all the Sn-isotopes. Also displayed is the parabolic fit to these energies, a quantity to be compared with $E_N = (\hbar^2/2I)(N - N_0)^2$, namely the energy associated with the members of the pairing rotational band. The difference with the spectrum of pair addition and subtraction modes displayed in Fig. 2.1.1 b) is again evident.

A simple estimate of the pairing rotational band moment of inertia is provided by the single j -shell model¹⁹, namely $(\hbar^2/2I) = G/4 \approx 25/(4N_0)$ MeV. This estimate turns out to be rather accurate. Certainly better than one can expect. On the other hand, one is reminded of the fact that we are discussing properties which specifically characterize a coherent state²⁰, namely $|BCS\rangle$.

Also reported in the inset of Fig. 2.1.3 are the integrated values of the measured absolute two-neutron transfer cross sections, quantities which are reproduced by the theoretical predictions within experimental errors (Fig. 2.1.6). In principle, one could have expected a sensible constancy of these cross sections (transitions) as the pairing rotational model implies a common intrinsic deformed state in gauge space, namely $|BCS\rangle$ (see Sect. 2.4.2). On the other hand, the number of Cooper pairs α'_0 which defines deformation in gauge space is rather small (≈ 6) and thus subject to conspicuous fluctuations ($\Delta\alpha'_0/\alpha'_0 \approx \sqrt{6}/6 \approx 0.4$). Fluctuations which also affect the two particle transfer absolute cross sections (because $\sigma \sim \alpha'^2_0$, one can expect fluctuations in σ of the order of 100%).

In keeping with the analogy discussed in Figs. 2.3.3 and 2.4.1 between pairing and quadrupole rotational bands, we note that in the electromagnetic decay of these last bands one expects, in the case of heavy nuclei, fluctuations of the order of $(\sqrt{250}/250)^2$, i.e. less than 1%. Within this context, the average value of the absolute experimental cross sections displayed in the inset of Fig. 2.1.3 is 1762 μb , while the average difference between experimental and predicted values is 94 μb (see Fig. 2.1.6)²¹. Thus, the discrepancies between theory and experiment are bound in the interval $0 \leq |1 - \sigma_{th}(i \rightarrow f)/\sigma_{exp}(i \rightarrow f)| \leq 0.09$, the average discrepancy being 5%.

¹⁹Brink, D. and Broglia (2005) App. H, and refs. therein.

²⁰See App. 3.E and Sect. 6.4; see also Potel et al. (2017).

²¹Potel, G. et al. (2013b).

$\leq 3 \text{ MeV}$.

In Fig. 2.1.4 the excited pairing rotational bands based on 0^+ pairing vibrational modes are displayed as a single band, and are associated with the average value of the 0^+ excited states with energy $\leq 3 \text{ MeV}$. The best parabolic fit is shown. Also given are the relative (p, t) absolute integrated cross sections normalized to the corresponding values of the ground state rotational band. The cross talk between bands is in all cases $\leq 8\%$, the single j -shell value estimate being²² 6%.

The above results underscore the fact that, at the basis of an operative coarse grained approximation to the nuclear many-body problem (within this context cf. App. I.D, in particular the discussion following Eq. (I.D.5)), one finds a judicious choice of the collective coordinates²³. In other words, pairing vibrations are elementary modes of excitation containing the right physics to restore gauge invariance through their interweaving with quasiparticle states. Within the framework of the above picture, one can introduce at profit a collective coordinate α_0 (order parameter; see Sect. 6.4.1) which measures the number of Cooper pairs participating in the pairing condensate, and define a wavefunction for each pair $(U'_v + V'_v a_v'^\dagger a_{\bar{v}}'^\dagger) |0\rangle$ (independent pair motion, BCS approximation, see Figs. 2.4.1, 2.4.2 and 2.4.3), adjusting the occupation parameters V_v and U_v (probability amplitudes that the two-fold, Kramer's-degenerate pair state (v, \bar{v}) , is either occupied or empty), so as to minimize the energy of the system under the condition that the average number of nucleons is equal to N_0 (the Coriolis-like force felt, in the intrinsic system in gauge space by the Cooper pairs, being equal to $-\lambda N_0$). Thus, $|BCS\rangle = \prod_{v>0} (U'_v + V'_v a_v'^\dagger a_{\bar{v}}'^\dagger) |0\rangle$ provides a valid description of the independent pair mean field ground state, and of the associated order parameter $a'_0 = \langle BCS | P'^\dagger | BCS \rangle = \sum_{v>0} U'_v V'_v$, $P'^\dagger = \sum_{v>0} a_v'^\dagger a_{\bar{v}}'^\dagger$ being the pair creation operator²⁴. It is then natural to posit that two-particle transfer reactions are specific to probe pairing correlations in many-body fermionic systems. Examples are provided by the Josephson effect²⁵ between e.g. metallic superconductors, and (t, p) and (p, t) reactions in atomic nuclei²⁶.

Within this context we now take the basic consequence of pairing condensation in nuclei regarding reaction mechanisms. For this purpose let us consider a *gedanken experiment* in which the superfluid target and the projectile can at best come in such weak contact that only single-nucleon transfer leads to a yield falling within the sensitivity range of the measuring setup. Because $(\hbar^2 / 2M\xi^2) / |E_{corr}| \approx 10^{-2}$, Cooper pairs in superfluid nuclei behave as particles of mass $2M$ over distances ξ , even in the case in which the NN -potential vanishes in the zone between the weakly overlapping densities of the two interacting nuclei. One then expects

²²Brink, D. and Broglia (2005) App. H.

²³In this connection, we quote allegedly from S. Weinberg: "In solving a problem you may choose to use the degrees of freedom you like. But if you choose the wrong ones you will be sorry".

²⁴cf. Bardeen et al. (1957a), Bardeen et al. (1957b), Schrieffer (1964), Schrieffer, J. R. (1973) and references therein.

²⁵Josephson (1962).

²⁶cf. e.g. Yoshida (1962), Broglia, R.A. et al. (1973), Bayman (1971), Glendenning, N. K. (1965), Bohr (1964), Hansen (2013) and Potel, G. et al. (2013a) and references therein.

Cooper pair transfer to be observed. Not only. One also expects that the associated absolute differential cross section contains, for the particular choice of mass number made and within the framework of the theory of quantum measurement, all the information needed to work out a comprehensive description of nuclear superfluidity.

Because $\alpha_0 \sim N(0)$, cross sections associated with the transfer of Cooper pairs between members of a pairing rotational band, are proportional to the density of single-particle levels quantity squared. As a consequence, absolute two-nucleon transfer cross sections are expected to be of the same order of magnitude than one-nucleon transfer ones, and to be dominated by successive transfer (see Sects. 3.2 and 3.3). These expectations have been confirmed experimentally and by detailed numerical calculations, respectively. The above parlance, being at the basis of the Josephson effect, reflects both one of the most solidly established results in the study of BCS pairing, and explains the workings of a paradigmatic probe of spontaneous symmetry breaking phenomena.

Due to the fact that, away from the Fermi energy pair motion becomes independent particle motion (see Sect. 2.4), one-particle transfer reactions like e.g. (d, p) and (p, d) can be used together with (t, p) and (p, t) processes, as valid tools to cross check pair correlation predictions (see Chapter 4). In particular, to shed light on the origin of pairing in nuclei: in a nutshell, the relative importance of the bare NN -interaction and the induced pairing interaction (within this context see Sect. 2.6 and Fig. 1.9.1).

While the calculation of two-nucleon transfer spectroscopic amplitudes and differential cross sections are, a priori, more involved to be worked out than those associated with one-nucleon transfer reactions, the former are, as a rule, more "intrinsically" accurate than the latter ones. This is because, in the case of two nucleon transfer reactions, the quantity (order parameter α'_0) which expresses the collectivity of the members of a pairing rotational band, reflects the properties of a coherent state ($|BCS\rangle$). In other words, it results from the sum over many contributions ($\sqrt{j_\nu + 1/2} U'_\nu V'_\nu$, see Sect. 2.4, also Sect. 6.4.1), all of them having the same phase. Consequently, the relative error decreases as the square root of the number contributions ($\approx N(0)\Delta \approx 4 \text{ MeV}^{-1} \times 1.4 \text{ MeV} \approx 6$ in the case of the superfluid nucleus ^{120}Sn).

There is a further reason which confers $\alpha'_0 = \sum_j (j + 1/2) U'_j V'_j$ a privileged position with respect to the single contributions $(j + 1/2) U'_j V'_j$. It is the fact that $\alpha'_0 = e^{2i\phi} \sum_j (j + 1/2) U_j V_j = e^{2i\phi} \alpha_0$ defines a privileged orientation in gauge space, α_0 being the order parameter referred to the laboratory system which makes an angle ϕ in gauge space with respect to the intrinsic system to which α'_0 is referred²⁷. In other words, the quantities α'_0 which measure the deformation of the superfluid nuclear system in gauge space, and the rotational frequency $\lambda = \hbar\phi$ in this space, and associated Coriolis force $-\lambda N_0$ felt by the nucleons referred to the body fixed frame, are the result of solving selfconsistently the BCS number $N_0 = \sum_{jm} V_j^2 =$

²⁷See Sect. 2.4.2, see Potel, G. et al. (2013b).

Check comment
Ben Bayman
bayman RB
19/04/16
7:09

It is of notice that typical values of $Z_\omega \approx 0.7$, while for nuclei along the stability valley bare and induced pairing contributions are about equal which, according to Eq. (2.2.2) implies $G' \approx G = v_p^{bare}$, as in the case of a non-renormalized situation. On the other hand the physics is radically changed, particles being a consistent fraction of the time in excited states coupled to collective vibrations, pairing acquiring a state dependence. *(formfactors)*

All of the above many-body, ω -dependent effects which imply in many cases a coherent sum of amplitudes, together with the corresponding renormalizations of the single-particle radial wavefunctions not discussed within the present framework, are not simple to capture in a spectroscopic factor³⁹ in connection with one-particle transfer, let alone two-nucleon transfer processes⁴⁰.

2.3 Quantality Parameter

The quantality parameter⁴¹ is defined as the ratio of the quantal kinetic energy of localization (confinement) and potential energy, (cf. Fig. 2.3.1 and Table 2.3.1). Fluctuations, quantal or classical, favor symmetry: gases and liquids are homogeneous. Potential energy on the other hand prefers special arrangements: atoms like to be at specific distances and orientations from each other (spontaneous breaking of translational and of rotational symmetry reflecting the homogeneity and isotropy of empty space⁴²).

When q is small, quantal effects are small and the lower state for $T < T_c$ will have a crystalline structure, T_c denoting the critical temperature. For sufficiently large values of $q (> 0.15)$ the system will display particle delocalization and, likely,

³⁹In keeping with the fact that $m_k \approx 0.6 - 0.7m$ and that $m^* \approx m$, as testified by the satisfactory fitting standard Saxon-Woods potentials provides for the valence orbitals of nucleons of mass m around closed shells, one obtains $m_\omega \approx 1.4 - 1.7m$. Thus $Z_\omega \approx 0.6 - 0.7$. It is still an open question how much of the observed single-particle depopulation can be due to hard core effects, which shifts the associated strength to high momentum levels (see Dickhoff, W. and Van Neck (2005), Jenning, B. (2011), Kramer, G. J. et al. (2001), Barbieri, C. (2009), Schiffer, J. P. et al. (2012), Duguet, T. and Hagen (2012), Furnstahl, R. J. and Schwenk (2010)). An estimate of such an effect of about 20% will not quantitative change the long wavelength estimate of Z_ω given above. Arguably, a much larger depopulation through hard core effects remains an open problem within the overall picture of elementary modes of nuclear excitation and of medium polarization effects. It remains an open question the role of the renormalization of the radial dependence of the single-particle wavefunctions due to many-body effects can play.

⁴⁰See Barranco et al. (2005, 1999).

⁴¹Nosanow (1976), de Boer (1957), de Boer (1948), de Boer and Lundbeck (1948), Mottelson (1998).

⁴²Within this general context the physics embodied in the quantality parameter is closely related to that which is at the basis of the classical Lindemann criterion (Lindemann (1910)) to measure whether a system is ordered (e.g. a crystal) or disordered (e.g. a melted system) (Bilgram (1987), Löwen, H. (1994), Stillinger and Stillinger (1990); Stillinger (1995)). The above statement concerning the competition between potential energy and fluctuations, is also valid for the generalized Lindemann parameter (Stillinger and Stillinger (1990), Zhou et al. (1999)), used to provide similar insight into inhomogeneous finite systems like e.g. proteins (aperiodic crystals Schrödinger, E. (1944), see also Ehrenfest's theorem (Basdevant and Dalibard (2005) pag. 138 see also App. 2.C).

constituents	M/M_n	$a(\text{cm})$	$v_0(\text{eV})$	q	phase($T = 0$)
${}^3\text{He}$	3	2.9(-8)	8.6(-4)	0.19	liquid ^{a)}
${}^4\text{He}$	4	2.9(-8)	8.6(-4)	0.14	liquid ^{a)}
H_2	2	3.3(-8)	32(-4)	0.06	solid ^{b)}
${}^{20}\text{Ne}$	20	3.1(-8)	31(-4)	0.007	solid ^{b)}
nucleons	1	9(-14)	100(+6)	0.4	liquid ^{a),c),d)}

Table 2.3.1: Zero temperature phase for a number of systems of mass M (M_n : nucleon mass), the first four depending on atomic interactions (range Å, strength meV), the last one referring to the atomic nucleus. a) delocalized (condensed), b) localized, c) non-Newtonian solid (cf. e.g. Bertsch (1988), de Gennes (1994)), that is, systems which react elastically to sudden solicitations and plastically under prolonged strain, d) paradigm of quantal, strongly fluctuating, finite many-body systems. Delocalization or less does not seem to depend much on whether one is dealing with fermions or bosons (Mottelson (1998) and refs. therein; cf also Ebran et al. (2014a), Ebran et al. (2014b), Ebran et al. (2013), Ebran et al. (2012)).

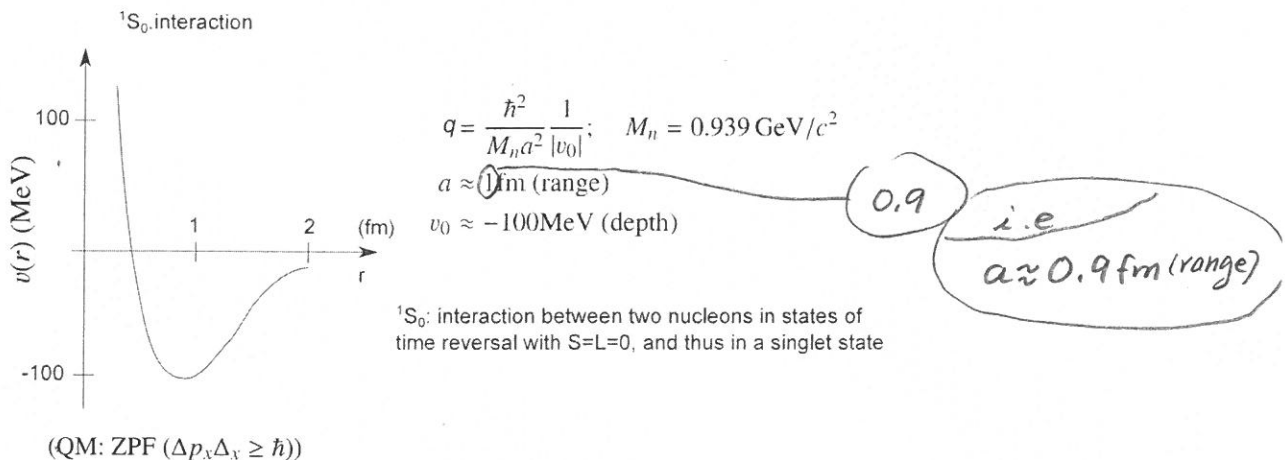


Figure 2.3.1: Schematic representation of the bare NN -interaction acting among nucleons displayed as a function of the relative coordinate $r = |\mathbf{r}_1 - \mathbf{r}_2|$, used to estimate the quantality parameter q , ratio of the zero point fluctuations (ZPF) of confinement and the potential energy.

Interplay between

i.e.

(Interplay between classical localization and quantal ZPF)

c) lower case

2.5. PAIR VIBRATION SPECTROSCOPIC AMPLITUDES

159

Classical localization and quantal ZPF

$$\delta x \delta k \geq 1$$

$$\varepsilon = \frac{\hbar^2 k^2}{2m}$$

$$\delta k = \frac{\delta \varepsilon}{\hbar v_F}$$

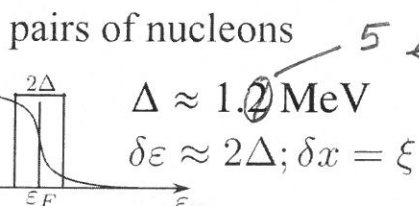
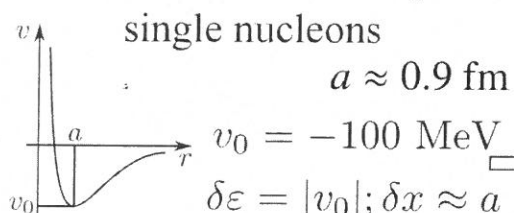
$$(v_F) \approx 0.27$$

(m)

structure

$$v_F/c$$

Independent motion of



quantality parameter

$$q = \frac{\hbar v_F}{\Delta} \approx 0.5 \ll 1$$

delocalization

$$\xi = \frac{\hbar v_F}{\Delta} \approx 14 \text{ fm} \gg R$$

$$q_g = \frac{\hbar^2}{2m\delta^2} \frac{1}{2\Delta} \approx 0.06$$

long range correlation

emergent property: generalized rigidy in
 3D-space

gauge space

? how does a short range force lead to
 single-nucleon mean free paths pairing correlations
 over distances

larger than nuclear dimension?

$$2R \approx 20/k_F$$

quantal

fluctuations phase correlations

(dominant mechanism)

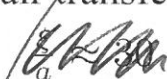
reactions

single particle transfer, e.g. (p,d)



the absolute cross section
 reflects the full renormalized
 nucleon transfer amplitude
 (energy, single-particle content,
 radial dependence of the
 wave function (form factor)).

Cooper pair transfer, e.g. (p,t)



(leaves space)

italics

Successive and simultaneous
 transfer amplitude contributions to
 the absolute cross section carry in a
 equal efficient manner information
 concerning pair correlations

Figure 2.4.2: Classical localization and zero point fluctuations, associated with independent-particle (normal density) and independent-pair (abnormal density).

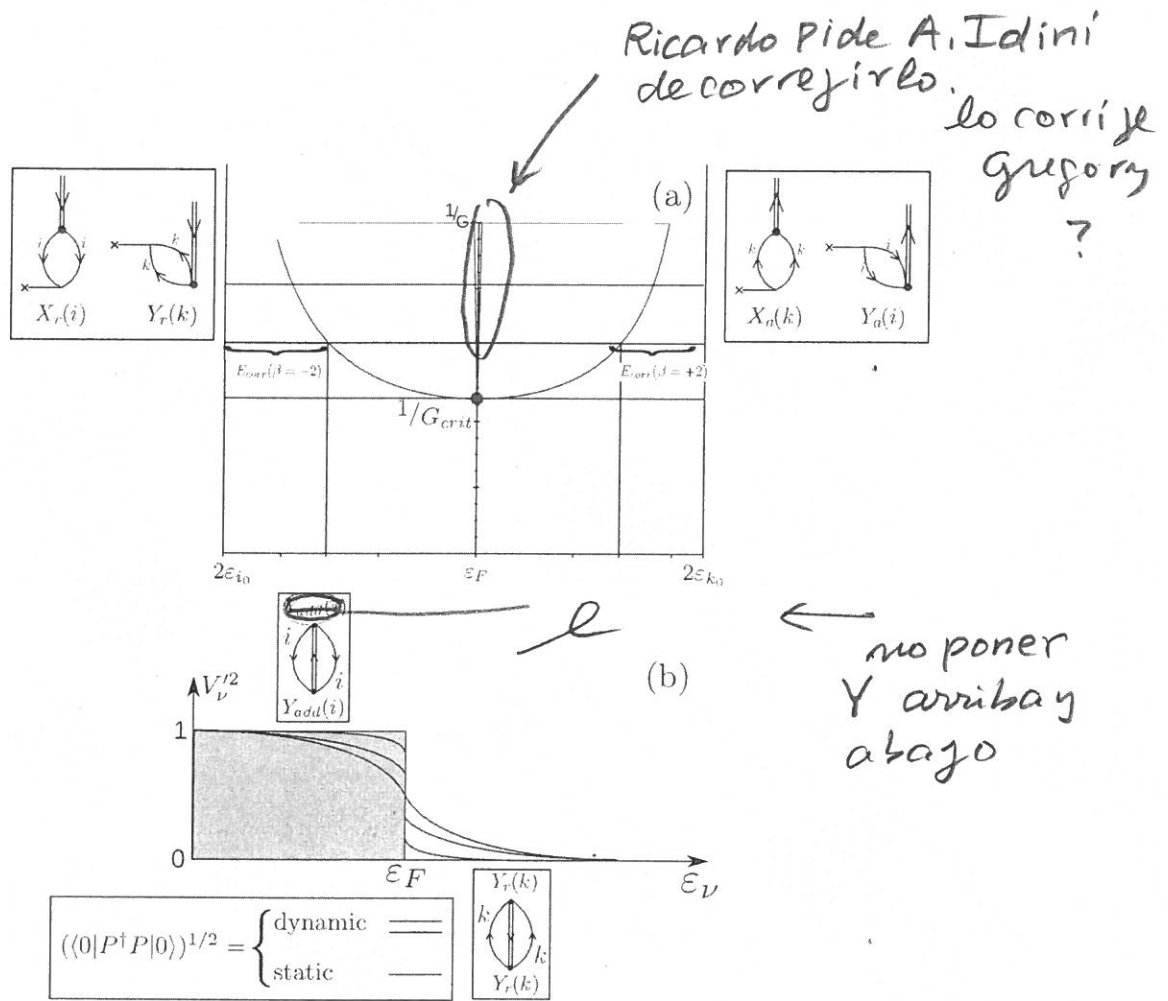


Figure 2.5.6: Schematic representation of the quantal phase transition taking place as a function of the pairing coupling constant in a (model) closed shell nucleus. (a) dispersion relation associated with the RPA diagonalization of the Hamiltonian $H = H_{sp} + H_p$ for the pair addition and pair removal modes. In the insets are shown the two-particle transfer processes exciting these modes, which testify to the fact that the associated zero point fluctuations (ZPF) which diverge at $G = G_{crit}$, blur the distinction between occupied and empty states typical of closed shell nuclei. (b) occupation number associated with the single-particle levels. For $G < G_{crit}$ there is a dynamical depopulation (population) of levels $i(k)$ below (above) the Fermi energy. For $G > G_{crit}$, the deformation of the Fermi surface becomes static, although with a non-vanishing dynamic component (cf. Fig. 2.1.2).

This result corresponds to the z -degree of freedom of the system (two H atoms at a distance $R \gg a_0$). One has thus to multiply the above result by 3 to take into account the x and y degrees of freedom. Thus

$$\Delta E^{(2)} = -\frac{6e^2 a_0^5}{R^6}. \quad (2.D.18)$$

Let us now calculate the van der Waals interaction between two H-atoms at a distance of the order of ten times the summed radii of the two atoms ($\approx 2a_0 \approx 1\text{\AA}$), that is for $R \approx 10\text{\AA}$,

$$\begin{aligned} \Delta E_{H-H}^{(2)}(10\text{\AA}) &\approx -\frac{6 \times 14.4 \text{ eV \AA}(0.529 \text{ \AA})^5}{(10 \text{ \AA})^6} \\ &\approx -3.6 \times 10^{-6} \text{ eV} = -3.6 \mu\text{eV} \end{aligned} \quad (2.D.19)$$

Making use of the relation

$$1 \text{ eV} = 2.42 \times 10^{14} \text{ Hz}, \quad (1 \text{ Hz} = \text{s}^{-1}) \quad (2.D.20)$$

one obtains

$$|\Delta E_{H-H}^{(2)}(10 \text{ \AA})| \approx 3.6 \times 10^{-6} \times 2.42 \times 10^{14} \text{ Hz} \approx 9 \times 10^8 \text{ Hz} \approx 10^3 \text{ MHz} \quad (2.D.21)$$

a quantity which can be compared with the Lamb shift (1058 MHz, Fig. 4.D.1; see also Fig. 6.2.1). It is of notice that $|\Delta E_{H-H}^{(2)}(2.5 \text{ \AA})| \approx 15 \text{ meV/part} \approx 0.35 \text{ kcal/mole}$, ($1 \text{ meV/part} \approx 0.02306 \text{ kcal/mole}$), a value of the order of $kT/2$. That is, one half of the thermal energy under biological conditions ($T \approx 300 \text{ K}$, $kT \approx 0.6 \text{ kcal/mole}$).*)

2.D.2 Critical dimension for van der Waals H-H interaction (protein folding domain)

Let us calculate the frequency associated with the $1s \rightarrow 2p$ transition ($=1 \text{ Ry}=13.6 \text{ eV}$),

$$\hbar\omega_e = 13.6 \text{ eV}. \quad (2.D.22)$$

Making use of

$$\hbar c = 2000 \text{ eV \AA}, \quad (2.D.23)$$

one can write

$$\omega_e = \frac{13.6 \text{ eV}}{\hbar c} c \approx 10^{-2} \text{ \AA}^{-1} c. \quad (2.D.24)$$

*) K. Huang, *Statistical Physics and Protein Folding*, World Scientific, Singapore (2005)

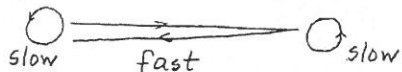


Figure 2.D.4: Schematic representation of the periodic motion associated with the hydrogen atom and the retarded van der Waals interaction.

Now; the exchange of “information” between the ZPF of the two H–atoms must be faster than the electronic revolution period, namely (Fig. 2.D.4)

$$\frac{2R}{c} \lesssim \frac{1}{\omega_e}. \quad (2.D.25)$$

Leading to $R < 50$ fm.

Otherwise the frequencies of the two periodic motions (ZPF based dipole–dipole interaction and orbiting of electron around proton) would be similar and strong coupling between them would take place. In other words, there would be a strong damping of the retarded, dispersive contribution to the van der Waals interaction.

In keeping with the fact that the linear dimensions of an amino acid are, in average, 0.36 nm, the typical distance between two residues in a protein in its native state is thus ≈ 10 Å. One would then expect that the maximum number of amino acids of globular protein or of a folding domain, to be of the order of $(50 \text{ \AA}/10 \text{ \AA})^3 \approx 125$ as empirically observed¹⁰⁶.

(do not break)

$$(50 \text{ \AA}/10 \text{ \AA})^3 \approx 125,$$

2.D.3 van der Waals between two amino acids

All of the commonly occurring amino acids in proteins have a central carbon atom (C_α) to which are attached a hydrogen atom, an amino group (NH_2), and a carboxy (COOH) (Fig. 2.D.5). What distinguishes one amino acid from another is the side chain attached to the C_α through its fourth valency. There are 20 different side chains specified by the genetic code. Amino acids are joined end to end during protein synthesis by the formation of peptide bonds. The carboxy group of the first amino acid condenses with the amino group of the next to eliminate water, thus the name residue, and yield a peptide bond.

The van der Waals interaction between two amino acids is,

$$\Delta E^{(2)} = -\frac{6Z^2 e^2 (a_0)^5}{R^6} \quad (2.D.26)$$

where Z is the number of protons of the molecule.

¹⁰⁶Rost (1997).

2.D.4 Average interaction between two side chains

Typical dimension of an amino acid is 0.36 nm ($=3.6 \text{ \AA}$). Let us then estimate the average van der Waals interaction of two residues at $R = 8 \text{ \AA}$. For this purpose use is made of $30 \leq Z \leq 35$. One can then write,

$$\begin{aligned}\Delta E_{aa}^{(2)} &= -\frac{6 \times Z^2 \times 14.4 \text{ eV } \text{\AA} (0.529 \text{ \AA})^5}{(8 \text{ \AA})^6} \\ &= \begin{cases} -12.3 \frac{\text{meV}}{\text{part}} = -0.28 \frac{\text{kcal}}{\text{mole}}, \\ -16.7 \frac{\text{meV}}{\text{part}} = -0.38 \frac{\text{kcal}}{\text{mole}}, \end{cases}\end{aligned}\quad (2.D.27)$$

Thus

$$\overline{\Delta E_{aa}^{(2)}}(8 \text{ \AA}) \approx -0.33 \frac{\text{kcal}}{\text{mole}} \quad (2.D.28)$$

a quantity to be compared to $kT = 0.6 \text{ kcal/mole}$.

Summing up, the van der Waals interaction between amino acids is weak, of the order of $kT/2 (\approx 0.3 \text{ kcal/mole})$, with a range $\lesssim 0.5 \text{ nm}$, and non-directional.

Hindsight

The van der Waals interaction is closely related to the restoration of spontaneous symmetry breaking of translational invariance (center of mass of finite systems like atoms and molecules define privileged positions in the otherwise homogeneous and isotropic vacuum), through ZPF of isoscalar and isovector character, some of which diverge although retaining a finite inertia (mass of the system) and associated emergent property, namely rigidity, pushing model; sloshing back and forth of opposite charges with very different spatial distributions (protons and electrons) thus essentially leading to a ground state displaying a low frequency dynamical dipole moment (See App. 1.D, discussion following Eq.(1.D.4)). Of notice that a similar phenomenon is found in atomic nuclei, in the case of light exotic halo neutron dripline systems like e.g. ^{11}Li (App. 2.B).

Appendix 2.E Phase transition and fluctuations¹⁰⁷

Empty space, considering also the quantal vacuum zero point fluctuations, is thought to be homogeneous and isotropic. Translational and rotational symmetry follows. But crystals, for example, of which all rocks are made, are neither homogeneous nor isotropic, displaying emergent properties like rigidity. Not only a crystal occupies and defines a fixed position and a privileged direction in space. Translational symmetry and isotropy is broken everywhere within it, in that the individual atoms

¹⁰⁷See e.g. Anderson and Stein (1984); Aderson (1976); Anderson (1964). For a short overview see Brink, D. and Broglia (2005) Ch. 1, p. 27. A more detailed account of the phenomenon is done in Ch. 6.

all occupy fixed positions and varied groups of them define particular directions. Lattice phonons are the corresponding fluctuations associated and restoring the broken symmetries by the individual atoms, while translation and rotation of the crystal is associated with symmetry restoration of the system as a whole.

Similarly, in a ferromagnetic crystal, where magnetization acquires a value different from zero below the Curie temperature breaking rotational invariance. In this case, spin waves are associated with symmetry restoration. In other words, another emergent property of spontaneous symmetry breaking –namely the fact that many–body systems can have ground states which do not have the same symmetry as the Hamiltonian itself– aside from (generalized) rigidity, is the existence of long–wavelength collective motions of the order parameter (amplitude of density waves in a crystal, magnetization in a ferromagnet, etc.), such as phonons and spin waves.

Superconductors break gauge symmetry, intimately related to charge and particle number conservation. A metallic superconductor has a rather perfect internal gauge phase order. Within this context, the BCS mechanism is most relevant to the mass problem because it introduces an energy (mass) gap for fermions, and the Goldstone–zero point motion of the total order parameter α_0 which is large and rapid ($\dot{\phi} = \lambda/\hbar$; pairing rotational bands in nuclei). Another major emergent property in broken symmetry systems is the appearance of singularities and texture of the order parameter like e.g. vortices in superfluid systems –namely, the possibility for a rotational invariant, spherical, quantal system to rotate (note van der Waals 1–Cooper pair in ^{11}Li , see Apps. 2.A and 6.F)– and of domain walls in ferromagnets.

Another feature of spontaneous symmetry braking (SSB) is the possibility of hierarchical¹⁰⁸ SSB or “tumbling”. Namely, SSB can be a cause for another SSB at a lower energy scale, an example being the chain crystal-phonon-superconductivity. Its Goldstone mode is the phonon (few meV) which induces the Cooper pairing of electrons ($T_c \approx 0.5$ meV) to cause superconductivity.

In the nuclear case, and in connection with the state $|^{11}\text{Li}(gs)\rangle$, one could argue that the incipient (dynamical) spontaneous symmetry breaking associated with the almost degeneracy of a soft dipole¹⁰⁹ mode, allows for an incipient breaking of gauge invariance at the level of a single Cooper pair ($S_{2n} \approx 380$ keV). The new feature in this case is the symbiotic character of the two incipient (dynamical) SSB phenomena.*)

2.E.1 Pairing phase transition in small particles

For bulk pure superconductors the large pair coherence length implies a very sharp, extremely narrow critical region as a function of the temperature (or of the magnetic field) so that, for example, the observed specific heat can be accurately described by the standard mean field BCS approach. However, the size of the critical

¹⁰⁸ See Nambu (1991).

¹⁰⁹ $E_x \lesssim 1$ MeV, long wavelength $\lambda = 2\pi R/L \approx 2\pi \times 4.58 \text{ fm}/l \approx 29 \text{ fm}$.

*)

region becomes larger as the dimensions of the system decreases below the coherence length. A limiting case corresponds to particles with dimensions smaller than the coherence length which form essentially zero-dimensional systems^{110,111}. An interesting question one may pose is for which size of particles will superconductivity actually cease. It was conjectured¹¹² that the usual Cooper instability will not exist anymore and therefore superconductivity should disappear if the small superconducting particles are in the quantum-size-effect (QSE) regime when the energy difference δ between two discrete one-electron states is comparable to the energy of the superconducting state (Anderson criterion). This means that small superconductors with fewer than about 10^4 to 10^5 electrons should be affected by this effect. Within this context, important information concerning pairing fluctuations is provided by the study of small Sn-particles at low temperatures¹¹³. To describe these fluctuations, use of techniques have been made that take into account large amplitude fluctuations of the order parameter. In particular the static-path approximation¹¹⁴ (SPA) with quadratic corrections¹¹⁵ which mimic the RPA corrections known to be, aside from a narrow interval around T_c (or H_c ; see Fig. 2.1.2), equivalent to number projection¹¹⁶. The relevant parameter of this sort of calculations is the ratio of δ and kT_c , i.e.

$$\bar{\delta} = \frac{\delta}{kT_c} = \frac{2}{N(0)kT_c}, \quad (2.E.1)$$

where $N(0)$ is the single-particle energy density of one spin orientation states at the Fermi energy. In Fig. 2.E.1 the results of the (SPA)+quadratic correction model for specific heat and spin susceptibility as a function of temperature is shown for $\bar{\delta}$ ranging from $\bar{\delta} = 0.001$ to $\bar{\delta} = 0.5$. The dashed curves show the static path results while the solid lines include the RPA-like corrections. For comparison, the BCS-results labeled by $\bar{\delta} = 0$ corresponding to the bulk system are also displayed.

For small values of $\bar{\delta}$ the system shows a sharp phase transition which can be well described by mean field theory. For $\bar{\delta} \approx 0.5$, corresponding to a small number of particles ($\sim 10^2$), the transition region has broadened so much as to blur the phase transition. RPA corrections are important only for relatively small particles.

¹¹⁰See Perenboom et al. (1981); Anderson (1959); Kubo (1962, 1968); Mühschlegel et al. (1972); Lauritzen et al. (1993).

¹¹¹An embodiment of such systems is provided by superfluid nuclei as a function of the rotational frequency (Fig. 2.1.2).

¹¹²Anderson (1959).

¹¹³Perenboom et al. (1981).

¹¹⁴Mühschlegel et al. (1972).

¹¹⁵Lauritzen et al. (1993). It is of notice that in Mühschlegel et al. (1972), the basic result of the work of the same authors (Denton et al. (1971)) on small normal-metal particles is mentioned to be the restriction to fixed electron number and the assertion is made that in the superconducting case (where they use the grand canonical ensemble) the above restriction to fixed electron number is expected to be even more important.

¹¹⁶Shimizu, Y. R. and Broglia (1990).